1

Theoretical Description of the Fourier Transform of the Absolute Amplitude Spectra and Its Applications

Levente Csoka and Vladimir Djokovic
[1]*University of West Hungary, Institute of Wood and Paper Technology, Bajcsy Zs. E. u. 4, 9400 Sopron,*
[2]*Vinca, Institute of Nuclear Science, P.O. Box 522, 11001 Belgrade*
[1]*Hungary*
[2]*Serbia*

1. Introduction

Speaking in a very broad sense, the Fourier transform (FT) can be treated as a systematic way to decompose arbitrary function into a superposition of harmonic ("symmetrical") functions. It is a fundamental tool for studying of various processes and for this reason it is present in basically every scientific discipline. In last decades, the Fourier transformation was used in distinctive fields such as geophysics (Maus 1999, Skianis et al. 2006), image decomposition in neuroscience (Guyader et al. 2004), imaging in medical applications (Lehmann et al., 1999) just to mention a few. Recently, FT was successfully applied in wood sciences (Fujita et al. 1996; Midorikawa et al. 2005, Midorikawa and Fujita 2005). For example, Fujita and co-workers (Midorikawa et al. 2005, Midorikawa and Fujita 2005) used two-dimensional Fourier transform method to analyze the cell arrangements within the xylem ground tissues. In our recent papers (Csoka et al. 2005, Csoka et al. 2007), we made one step forward and try to analyze the wood anatomy via FT of the density function of the tree. Method is based on a forwarded Fourier transformation of the absolute amplitude spectra. Since the comprehensive literature survey of the accessible studies did not reveal any similar results based on this method, in this chapter we will discuss the basic theorem of FT of an absolute amplitude spectrum and a possibility to generate higher order FT defined as,

$$\left\langle F\left[f(x)\right](k)\right\rangle^{th}. \tag{1}$$

The discussion also includes a brief description of the theory of the forwarded FT of the complex and absolute amplitude spectrum found in the literature. In the second part of the chapter, it will be shown how the presented theory can be applied to the analysis of the wood anatomy, specifically to determination of the transition point between juvenile and mature wood.

2. Problem statement

We will start these theoretical considerations with familiar one-dimensional Fourier transform (FT) of a given function $f(x)$,

$$F(k) = F[f(x)](k) = \int_{-\infty}^{\infty} f(x) e^{-i2\pi xk} dx, \tag{2}$$

where $F(k)$ is referred to as the spectrum of $f(x)$. The absolute amplitude spectrum of $F(k)$ is defined as,

$$\left|\{F(k)\}\right| = \sqrt{\Re\{F(k)\}^2 + \Im\{F(k)\}^2}\ . \tag{3}$$

Depending on the particular problem, the amplitude spectrum of a signal can be treated as complex or absolute function.

As it was stated in the introduction, the main topic of this chapter is the Fourier transform of the absolute amplitude spectrum and its application to analysis of the wood anatomy. For this reason, we will first consider two basic methods for calculation of the forwarded FT of the amplitude function. The first method is to transform the complex amplitude spectrum $F[f(x)]$ again according to Eq. (2). The second approach is to calculate Fourier transform on the absolute amplitude spectrum via so-called *Wiener-Khinchin* theorem.

2.1 Fourier transform of the complex amplitude spectrum

In the case when the complex amplitude spectrum is transformed the result is a time/space function which has been mirrored with respect to the y-axis, or,

$$f(x) \xrightarrow{FT} F(k) \text{ then } F(k) \xrightarrow{FT} f(-x)\ . \tag{4}$$

The theoretical exposition of Eq. (4) in discrete considerations is as follows. Let the basic finite interval be [0,1]. If we divide that interval in N equal parts, we will obtain $\left\{\frac{k}{N} : k = 0,...,N-1\right\}$ points. Let the value at k point be $f(k)$. From the practical reasons we will select the discrete basis $\left\{ e_j : j = 0,...,N-1\right\}$, where

$$e_j(k) = \frac{1}{\sqrt{N}} e^{2\pi ij\frac{k}{N}}\ . \tag{5}$$

The $\frac{1}{\sqrt{N}}$ coefficient is necessary, because of the normalization. Now, the discrete FT of f is,

$$F(f)(j) = \frac{1}{\sqrt{N}} \sum_{k=0}^{N-1} f(k) e^{-2\pi ij\frac{k}{N}} \qquad (j = 0,...,N-1)\cdot \tag{6}$$

Performing the FT on the obtained $F(f)$:

$$F(F(f))(l) = \frac{1}{\sqrt{N}} \sum_{j=0}^{N-1} F(f)(j) e^{-2\pi il\frac{k}{N}} = \tag{7}$$

$$= \frac{1}{\sqrt{N}} \sum_{j=0}^{N-1} \left(\frac{1}{\sqrt{N}} \sum_{k=0}^{N-1} f(k) e^{-2\pi i l \frac{k}{N}} \right) e^{-2\pi i l \frac{k}{N}} = \tag{8}$$

$$= \frac{1}{N} \sum_{k=0}^{N-1} f(k) \sum_{j=0}^{N-1} e^{-2\pi i j \frac{k}{N}} e^{-2\pi i l \frac{k}{N}} = \tag{9}$$

$$= \frac{1}{N} \sum_{k=0}^{N-1} f(k) \sum_{j=0}^{N-1} e^{-2\pi i k \frac{j+l}{N}} \quad (j = 0,...,N-1) \tag{10}$$

The sum of a geometric series of the first N member,

$$\sum_{j=0}^{N-1} e^{-2\pi i k \frac{i+l}{N}} \tag{11}$$

is 0, if

$$j + l \neq 0. \tag{12}$$

If

$$j + l = 0, \tag{13}$$

that is

$$j = -l\,, \tag{14}$$

then,

$$F\left(F(f)\right)(l) = f(-l)\,. \tag{15}$$

2.2 Fourier transform of the absolute amplitude spectrum

The estimation of the Fourier transform of the absolute values of the amplitude spectrum, $\left|\{F(k)\}\right|$, requires different approach. In order to find the FT of the absolute spectrum,

$$F_k(|F(k)|)(\ell)\,, \tag{16}$$

it is necessary to use the *Wiener-Khinchin* theorem,

$$F_k[|F(k)|^2](\ell) = \int_{-\infty}^{\infty} \overline{f}(\tau) f(\tau + \ell) d\tau, \tag{17}$$

where $\overline{f}$ denotes the complex conjugate of f (by definition Eq. (17) is a relationship between FT and its autocorrelation function).
Using Eq. (17), $\left|F(k)\right|$ can be expressed as,

$$|F(k)| = \sqrt{\int_{-\infty}^{\infty} \left[F[|F(k)|^2](\ell) \right] e^{i2\pi k \ell} d\ell} = \tag{18}$$

$$= \sqrt{\int_{-\infty}^{\infty}\left[\int_{-\infty}^{\infty}\overline{f}(x)f(x+\ell)dx\right]e^{i2\pi k\ell}d\ell}\ . \tag{19}$$

Therefore, the Fourier transform of the absolute amplitude spectrum is

$$F[\,|F(k)|\,](\ell) = \int_{-\infty}^{\infty}|F(k)|\ e^{-i2\pi k\ell}dk \tag{20}$$

$$= \int_{-\infty}^{\infty}\sqrt{\int_{-\infty}^{\infty}\left[\int_{-\infty}^{\infty}\overline{f}(x)f(x+\tilde{\ell})dx\right]e^{i2\pi k\tilde{\ell}}d\tilde{\ell}}\ \ e^{-i2\pi k\ell}dk \tag{21}$$

Spectrum presented by Eq. (21) is essentially different from that of Eq. (4). However, neither Eq. (21) nor Eq. (4) was suitable in our attempt to draw additional information from the experimentally determined density function of the tree stem e.g. to determine the transition point between juvenile and mature wood. As it will be seen below, it turned out that in this practical case it is necessary to perform additional forwarded FT to the positive half of the absolute amplitude spectrum only. In the following section we will consider the forwarded FT of the absolute amplitude spectrum which originates from the superposition of a multitude of harmonic signals.

3. The forwarded FT of the absolute amplitude spectrum which consists of a multitude of harmonic signals

We will start the analysis of the forwarded FT of the absolute amplitude spectrum by considering monochromatic functions obtained by Dirac delta segment sampling of a continuous signal. If $x(t)$ is a original continuous signal then the sampled discrete function, $x_s(t)$, is given by

$$x_s(t) = x(t)(T\ \Delta_T(t))\ , \tag{22}$$

where $\Delta_T(t)$ is the sampling Dirac delta operator and T is the period. Taking that Fourier series of $\Delta_T(t)$ is,

$$\sum_{k=-\infty}^{\infty} e^{i2\pi k f_s t}\ , \tag{23}$$

Eq. (22) can be written as:

$$x_s(t) = \sum_{k=-\infty}^{\infty} x(t)e^{i2\pi k f_s t}\ , \tag{24}$$

where f_s is the sampling frequency and the principle frequency of the periodicity of $\Delta_T(t)$. The amplitude spectrum of monochromatic function given by Eq. (24) can be represented by one dimensional Dirac delta function pair:

$$\delta(f - f_s) + \delta(f + f_s)\,. \tag{25}$$

If the signal is sampled at f_s samples per unit interval, the FT of the sampled function is periodic by a period of f_s.

Let us consider a finite length segment of $x_s(t)$ by performing an L length rectangle window function $\prod(x)$, which is 0 outside the L interval and unity inside it. The FT of a rectangle window function is given by

$$F_x[\prod(x)](k) = \int_{-\infty}^{\infty} e^{-i2\pi kx} \prod(x)\, dx = \sin c(\pi k)\,. \tag{26}$$

Fourier transform of the $x_s(t)$ $\prod(x)$ product is a convolution operation, which allows us to calculate the spectrum of the windowed, finite function:

$$F[x_s(t)\prod(x)] = F[x_s(t)] * F[\prod(x)] = \delta(f \pm f_s) + \sin c(\pi k)\,. \tag{27}$$

It can be clearly seen that this convolution spectrum consists of a $\sin c(\pi k)$ set at the impulse-position of the Dirac delta function. If the $\prod(x)$ is positioned between $-L/2$ and $+L/2$ then the convolution's spectrum will contain real amplitude values only. Let us chose the length of the original $\prod(x)$ in such way that it contains the whole period of $x_s(t)$. In that case the convolution amplitude spectrum will be reduced to a Dirac delta function pair $\delta(f - f_s)$ and $\delta(f + f_s)$. For further considerations the positive frequency interval $[0,\, f_S/2]$ is taken which contains single Dirac delta function $\delta(f - f_s)$. That is achieved by multiplication of the amplitude spectrum in the frequency space with window $\prod(k)$ function. The $\prod(k)$ function is not symmetric at the centre; it is shifted to positive direction by one quarter of the original sampling frequency. Finally, the Fourier transform of the obtained $\delta(f - f_s)$ function is an exponential function:

$$F[\delta(f - f_s)] = \sum \delta(f - f_s) e^{-i2\pi f_s k} = e^{-i2\pi f_s k} \tag{28}$$

and its amplitude spectrum is unity,

$$\cos(2\pi f_0 x) \Rightarrow \left| e^{-i2\pi f_0 \ell} \right| = 1\,. \tag{29}$$

When, however, $x_s(t)$ is a superposition of more harmonic signals, the sum,

$$\sum_j \cos(2\pi f_{0j} x) \Rightarrow \left| \sum_j e^{-i2\pi f_{0j} \ell} \right|, \tag{30}$$

is generally not unity, but it exhibits oscillations. The former result suggests the presence of the complex interaction between amplitude waves which can be used in order to draw the additional information from the original signal. It should be noted that the performing of the FT on the absolute amplitude spectrum will give the spectrum with an argument that is expressed in the same dimensional units as the variable of the original spectrum. For this reason, we believe that the interference peaks in the forwarded FT of the absolute spectrum carry information about the specific positions where certain processes were activated, which, otherwise, can not be observed directly in the original spectrum. Reciprocate of Eq. (30) was further used to determine the FT spectrum of the absolute amplitude spectrum from a density function of a tree. Similarly to Eq. (30) we can generate formula for two dimensional signals (pictures) as,

$$\sum_m \sum_n \cos(2\pi f_{0m} x) \cos(2\pi f_{0n} x) \Rightarrow \left| \sum_m \sum_n e^{-i2\pi f_{0m} \ell} e^{-i2\pi f_{0n} \ell} \right|. \tag{31}$$

It should also be emphasized that if the sum in Eq. 30 is different from unity then it will be possible to generate higher order FT of the absolute amplitude spectrum.

4. Examples and discussion

Timber is a biosynthetic end product so the making of wood is a function of both gene expression and the catalytic rates of structural enzymes. Thus, to achieve a full understanding of wood formation, each component of the full set of intrinsic processes essential for diameter growth (i.e. chemical reactions and physical changes) must be known, investigate in complex form and information on how each one of those components is affected by other processes (Savidge et al., 2000).

The younger juvenile wood produced in the crown has features which distinguish it from the older, more mature wood of the bole (Zobel and Sprague, 1999). Variations within a species are caused by genetic differences and regional differences in growth rate. Differences also occur between the juvenile and mature wood within single trees, and between the earlywood (springwood) and latewood (summerwood) within each annual growth ring. Juvenile wood is an important wood quality attribute because depending on species, it can have lower density, has shorter tracheids, has thin-walled cells, larger fibrial angle, and high – more than 10% – lignin and hemicellulose content and slightly lower cellulose content than mature wood (Zobel and van Buijtenen, 1989, Zobel and Sprague, 1999). Wood juvenility can be established by examining a number of different physical or chemical properties.

Juvenile wood occupies the centre of a tree stem, varying from 5 to 20 growth rings in size, and the transition from juvenile to mature wood is supposed to gradual. This juvenile wood core extends the full tree height, to the uppermost tip (Myers et al., 1997). It is unsuitable for many applications and has great adverse economic impact. Juvenile wood is not desirable for solid wood products because of warpage during drying and low strength properties and critical factors in producing high stiffness veneer (Willits et al., 1997). In the other hand, in the pulp and paper industry juvenile wood has higher than mature wood in tear index, tensile index, zero-span tensile index, and compression strength. For the same chemical pulping conditions, pulp yield for juvenile wood is about 25 percent less than pulp yield for mature wood (Myers et al., 1997).

It is, therefore, important from scientific as well as from practical reasons to determine the demarcation line between juvenile and mature wood. The advantage of the present approach that this boundary line can be determined by analysis of density spectrum which was obtained by non-invasive X-ray densitometry method.

4.1 Materials and methods

Twelve selected trees were investigated, which were planted in Akita Prefectures, Japan. The name of the tree is sugi (Cryptomeria japonica D. Don). The trees were harvested in different ages between 71 and 214 years (Table 1). Tracheid lengths, annual ring structure, were also determined from those samples.

4.2 X-ray densitometry

Bark to bark radial strips of 5 mm thickness were prepared from the air-dried blocks cut from the sample disks. After conditioning at 20 °C and 65% RH, without warm water

extraction, the strips were investigated by using X-ray densitometry technique, with 340 seconds of irradiation time. The current intensity and voltage were 14 mA and 17 kV, respectively. The distance between the X-ray source and the specimen was 250 cm. The developed films were scanned with a densitometer (JL Automation 3CS-PC) to obtain density values across the growth rings (Figure 1) and with a table scanner (HP ScanJet 4C) to obtain digital X-ray picture for image processing.

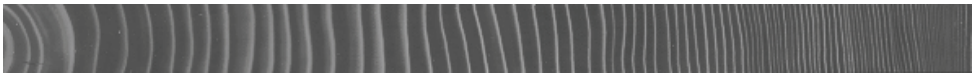

Fig. 1. X-ray image of a sugi sample

The growth ring parameters of ring width (RW), minimum density within a ring (D_{min}), maximum density within a ring (D_{max}) and ring density (RD: average density within a ring) were determined for each growth ring by a special computer software. The latewood is categorized by Mork's definition, as a region of the ring where the radial cell lumens are equal to, or smaller than, twice the thickness of radial double cell walls of adjacent tracheids (Denne, 1989). A threshold density, 0.55 g/cm^3 was used as the boundary between earlywood and latewood (Koizumi et al., 2003).

4.3 FT of the density function of the sugi tree

Figure 2 shows density function of the sugi tree obtained by laser scanning of the x-ray image. It can be seen that the signal is periodic and its amplitude FT spectrum is shown in Figure 3. The amplitude spectrum shows a strong peak at frequency 0.4 mm^{-1} which shows that the most frequent annual ring is about 2.5 mm. However, after reciprocate of the Eq. (34) was used in order to determine the spectrum of the absolute amplitude spectrum some additional information were obtained (Figure 4). While the amplitude spectrum shows the frequency structure of continuous or discrete signals, the forwarded FT of the absolute amplitude spectrum can provide the information about the complex effect of the interaction among these waves.

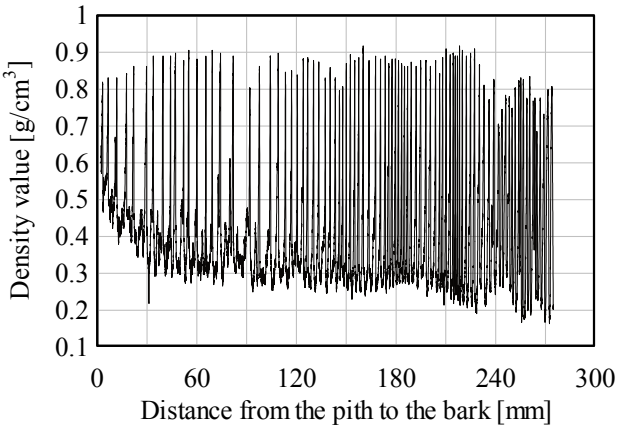

Fig. 2. The density function of a sugi tree (obtained by laser scanning of the X-ray image)

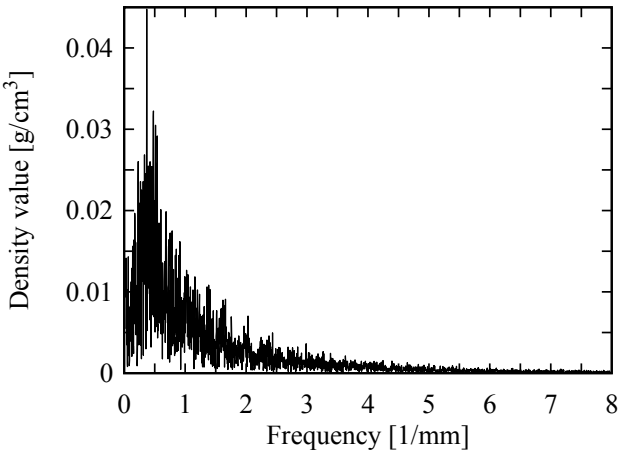

Fig. 3. The amplitude spectrum of the density function

As it can be noticed in Figure 4, the second FT spectrum shows spikes at certain positions. These peaks suggest the locations in the original complex function where the superposition of two or more periodic curves takes place. The highest peak has been assigned to the transition point between juvenile and mature wood (Csoka et al., 2007). Note that FT changes the dimension of the independent variable according to the input signals. The dimension of the variable of the second FT spectrum is the same as the dimension of the original variable. It should also be emphasized that the obtained values for the transition between juvenile and mature wood calculated from the second FT spectrum were in agreement with the values obtained from segmented model of tracheid lengths (Zhu et al., 2005).

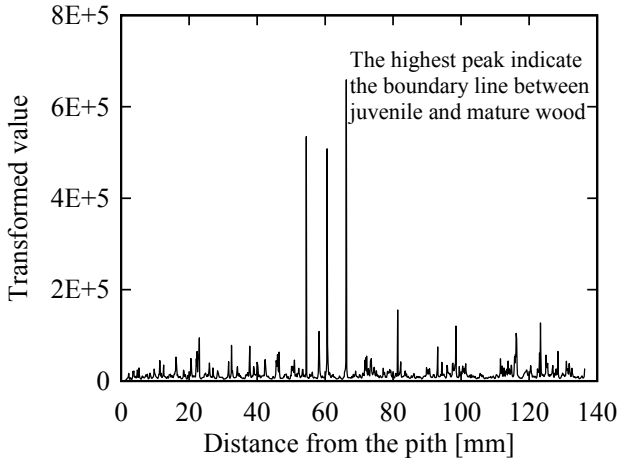

Fig. 4. The forwarded FT of the amplitude spectrum of a density function

The variables and typical parameters of the density function, its amplitude spectrum and the Fourier transform of the amplitude spectrum are given in *Table 1*. In that table L represents the actual length of the sample which depends of the age of the wood. However, increment between discrete points is kept constant to 0.015 mm. It should be also pointed out that one annual ring is represented by 200-400 points.

Properties of spectrums		
density function	*Amplitude spectrum*	*FT of amplitude spectrum*
length of x axis	length of the x axis	length of the x axis
$L \quad [mm]$	$f_s / 2 = 33.3\dot{3} \quad [1/mm]$	$L/2 \quad [mm]$
increment between points	increment between points	increment between points
$\Delta l = L/N = 0.015\,[mm]$	$\Delta l = L_1/N_1$	$\Delta l = L_2/N_2$
number of points	number of points	number of points
N	$N/2$	$N/4$

Table 1. The variables and typical parameters of the density function, its amplitude spectrum and the Fourier transform of the amplitude spectrum

4.4 FT of the X-ray image

X-ray image (Figure 1) was first processed by using a spatial grey level method. After the determination of the grey level at each point in the image, a 2D power spectrum that represents image in the frequency domain was calculated via Fourier transformation. Figure 5 shows the obtained power spectrum in a 3D representation. The amplitude spectrum of an X-ray image expresses a function (which is a point in some infinite dimensional vector space of functions) in terms of the sum of its projections onto a set of basis functions. The amplitude spectrum of the image carries information about the relative weights with which frequency components (projections) contribute to the spectrum, while the phase spectrum (not shown) localizes these frequency components in space (Fisher et al., 2002). It should be noted that in the Fourier domain image, the number of frequencies corresponds to the number of pixels in the spatial domain image, i.e. the image in the spatial and Fourier domains are of the same size (Castleman 1996).

The 3D representation of the power spectrum in Figure 5 is related to the rate at which gradual brightness in the X-ray image varies across the image. The frequency refers to the rate of repetitions per unit time i.e. the number of cycles per millimetre. Therefore, the intensive peaks observed in Figure 5 indicate the basic frequencies of the annual ring pattern in the frequency domain. The forwarded FT of the amplitude spectrum of the image is shown in Figure 6. With a closer look at the original image, a strong relationship between the annual ring texture and the spectrum in Figure 6 can be noticed, with could also justify our approach of using forwarded Fourier transformation of the absolute spectrum for determination of the demarcation zone between juvenile and mature wood. The texture of the 3D picture obtained from the forwarded FT of the absolute spectrum exhibit obvious annual ring pattern.

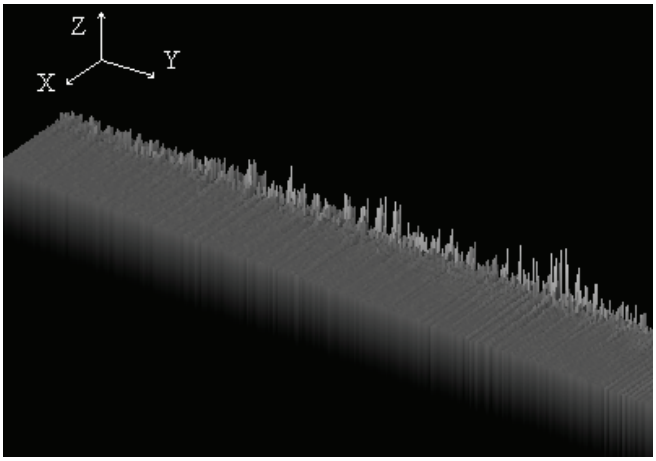

Fig. 5. The power spectrum of the X-ray image (Figure 1) in 3D representation

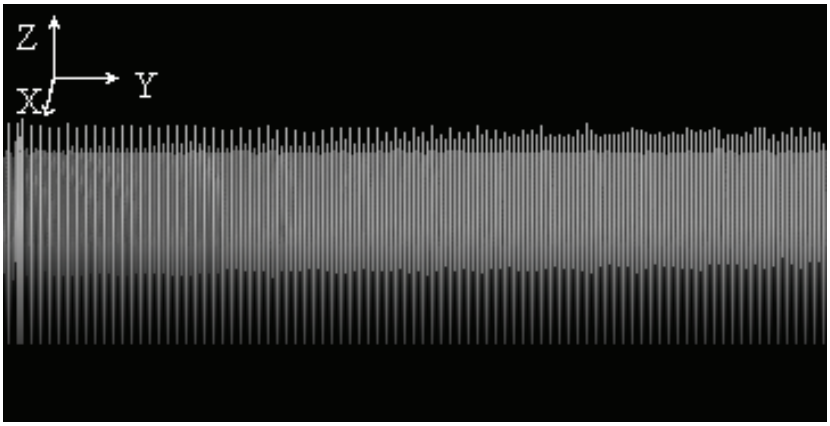

Fig. 6. The forwarded FT of the amplitude spectrum of the X-ray image

In order to analyze to transition between juvenile and mature wood from the forwarded FT of the amplitude spectrum of X-ray image, horizontal intensity line slices have been took through the spectrum in Figure 6. This pixel slice contains information about

possible interactions between certain modes in the amplitude spectrum. The spectrum in Figure 7 was obtained by taking the sum of the slices from the bottom to the top of the image. The highest peak in the spectrum refers to the transition point of juvenile and mature wood.

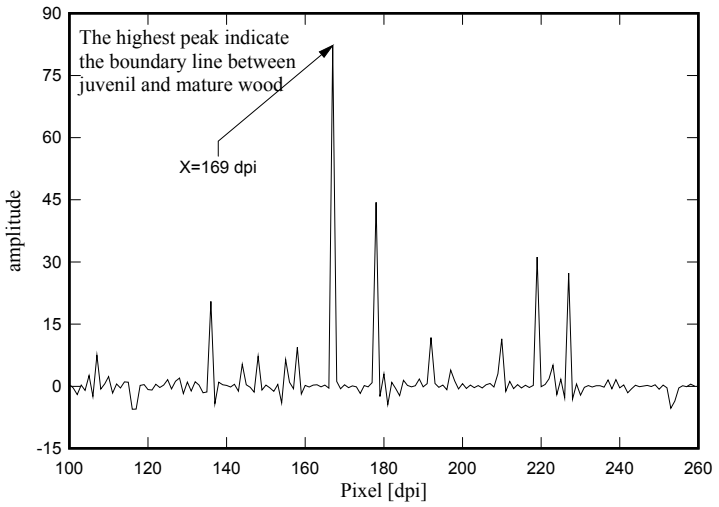

Fig. 7. The sum of pixel slices from the bottom to the top of the forwarded FT of the amplitude spectrum presented in Figure 6

5. Conclusions

Since the determination of the boundary zone between juvenile and mature wood is a subject of great practical importance in the area of wood anatomy, a various methods were suggested to address this problem. However, most of these methods considered only a limited number of characteristic features of the wood stem (one or two). For example, for a long time, the researchers were focused on the measurements of the annual ring width, the specific gravity, tracheid length and microfibril angle (Fujisaki 1985, Fukazawa 1967, Matyas and Peszlen 1997, Ota 1971, Yang et al. 1986, Zhu et al. 2000). The method based on the nonlinear, segmented regression method of tracheid length and microfibril angle (Cook and Barbour 1989, Zhu et al. 2005) has provided a common and simple tool for analyzing of the growth variation, while at the same time it was not restricted to certain groups of species or types of data. Unfortunately, all these different approaches did not take the complexity of the stem into account. The global nature of the above mentioned processes hides local density-distribution information, and makes the determination of the changes related to the distance from the pith impossible.

In this chapter we presented the FT of an amplitude spectrum theorem that can find direct application in studying of a wood anatomy. In spite of its simplicity, to our best knowledge there is no reference in the literature regarding the use of forwarded FT of the absolute amplitude spectra of an arbitrary vibration in the way we suggested. The suggested theoretical approach was used in order to determine the demarcation zone between juvenile and mature wood within a tree stem from the experimentally obtained density spectrum. The main advantage of the present method is that it enables simultaneous study of the changes in the density of annual rings and their distances from the pith, while they were, so far, studied as independent properties. The density function contains inherent information about changes in successive annual rings that may, after an appropriate mathematical analysis procedure, be used to describe the microstructure of the wood. It is assumed that the variation in the biological and physical characteristics of the cell (i.e. the cell dimension, the thickness of cell wall, the cellulose and lignin contents in the cell wall, and the growth rate) will be reflected in the sequences of wood density in the radial direction. The forwarded FT of the absolute amplitude spectrum provides information about the interaction of the amplitude waves, which can be further used to characterize the physical growth of the trees.

6. References

Denne, M.P. (1989). Definition of latewood according to Mork (1928). *International Association of Wood Anatomists Bulletin*. 10,1,59–62

Divos, F., Denes, L., Iniguez, G. (2005). Effect of cross-sectional change of a board specimen on stress wave velocity determination. *Holzforschung*. 59, 230-231

Cook, J.A., Barbour, R.J. (1989). The use of segmented regression analysis in the determination of juvenile and mature wood properties. *Report CFS No. 31. Forintek Canada*, Corp., Vancouver, BC

Csoka, L., Divos, F., Takata, K. (2007). Utilization of Fourier transform of the absolute amplitude spectrum in wood anatomy. *Applied Mathematics and Computation*. 193, 385-388

Csoka, L., Zhu, J., Takata, K. (2005). Application of the Fourier analysis to determine the demarcation between juvenile and mature wood. *J. Wood Sci.* 51, 309-311, 385-388

Fujisaki, K. (1985). On the relationship between the anatomical features and the wood quality in the sugi cultivars (1) on cv. Kumotoshi, cv. Yaichi, cv. Yabukuguri and cv. Measa (in Japanese). *Bull. Ehime Univ. Forest*. 23:47-58

Fujita, M., Ohyama, M., Saiki, H. (1996). Characterization of vessel distribution by Fourier transform image analysis. In: Lloyd AD, Adya PS, Brian GB, Leslie JW (eds) Recent advances in wood anatomy. Forest Research Institute, New Zealand, pp 36–44

Fukazawa, K. (1967). The variation of wood quality within a tree of Cryptomeria japonica – characteristics of juvenile and adult wood resulting from various growth conditions and genetic factors. *Res. Bull. Fac. Agric. Gifu Univ*. Japan, 25:47-127

Guyader, N., Chauvin, A., Peyrina, C., Hérault, J. Marendaz, Ch. (2004). Image phase or amplitude? Rapid scene categorization is an amplitude-based process *C. R. Biologies*. 327, 313–318

Koizumi, A., Takata, K., Yamashita, K., Nakada, R. (2003). Anatomical characteristics and mechanical properties of Larix Sibirica grown in South-central Siberia. *IAWA Journal*. 24, 4, 355-370

Lehmann, T.M., Gönner, C., Spitzer, K. (1999). Survey: Interpolation Methods in Medical Image Processing. IEEE *Transactions On Medical Imaging*. 18, 11, 1049-1075

Maus, S. (1999). Variogram analysis of magnetic and gravity data. *Geophysics.* 64, 3, 776-784

Midorikawa, Y., Ishida, Y., Fujita, M. (2005). Transverse shape analysis of xylem ground tissues by Fourier transform image analysis I: trial for statistical expression of cell arrangements with fluctuation. *J. Wood Sci*. 51, 201–208

Midorikawa, Y., Fujita, M. (2005). Transverse shape analysis of xylem ground tissues by Fourier transformimage analysis II: cell wall directions and reconstruction of cell shapes. J. Wood Sci. 51, 209–217

Matyas, C., Peszlen, I., (1997). Effect of age on selected wood quality traits of poplar clones. *Silvae Genetica*. 46, 64-72

Myers, G.C., Kumar, S., Gustafson, R.R., Barbour. R.J., Abubakr, S. (1997). Pulp quality from small-diameter trees. *Role of Wood Production in Ecosystem Management Proceedings of the Sustainable Forestry Working Group* at the IUFRO All Division 5 Conference, Pullman, Washington

Ota, S. (1971). Studies on mechanical properties of juvenile wood, especially of sugi-wood and hinoki-wood (in Japanese). *Bull. Kyushu Univ. Forests.* 45:1-80

Savidge, R.A., Barnett, J.R., Napier, R. /edited/ (2000). Cell and Molecular Biology of Wood Formation. BIOS, Biddles Ltd, Guilford, UK pp.2-7

Skianis, G.A., Papadopoulos, T.D., Vaiopoulos, D.A. (2006). Direct interpretation of self-potential anomalies produced by a vertical dipole. *Journal of Applied Geophysics*. 58, 130–143

Willits, S.A., Lowell, E.C., Christensen, G.A. (1997). Lumber and veneer yield from small-diameter trees. *Role of Wood Production in Ecosystem Management Proceedings of the Sustainable Forestry Working Group* at the IUFRO All Division 5 Conference, Pullman, Washington

Zhu, J., Nakano, T., Hirakwa, Y., Zhu, J.J. (2000). Effect of radial growth rate on selected indices of juvenile and mature wood of the Japanese larch. *J. Wood. Sci.* 46:417-422

Zhu, J., Tadooka, N., Takata, K., Koizumi, A. (2005). Growth and wood quality of sugi (*Cryptomeria japonica*) planted in Akita prefecture (II). Juvenile/mature wood determination of aged trees. *J. Wood Sci.* 51, 95-101

Zobel, B.J., van Buijtenen, J.R. (1989). *Wood variation, its cause and control*. p 375, Springer-Verlag, ISBN 354050298X, Berlin

Zobel, B., Sprague, J. R. (1998). *Juvenile wood in forest trees.* p 300, Springer-verlag, ISBN 3540640320, Berlin, Heidelberg

Yang, K. C., Benson, C., Wong J.K. (1986). Distribution of juvenile wood in two stems of Larix laricina. *Can J For Res.* 16:1041-1049

Yeh, T.F., Goldfarb, B., Chang, H.M., Peszlen, I., Braun, J.L., Kadla, J. F. (2005). Comparison of morphological and chemical properties between juvenile wood and compression wood of loblolly pine. *Holzforschung*. 59, 669-674

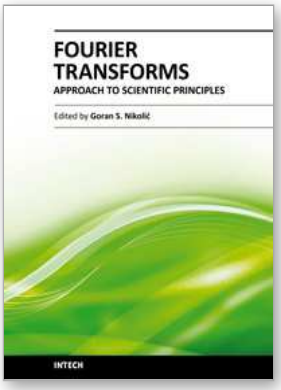

Fourier Transforms - Approach to Scientific Principles

Edited by Prof. Goran Nikolic

ISBN 978-953-307-231-9
Hard cover, 468 pages
Publisher InTech
Published online 11, April, 2011
Published in print edition April, 2011

This book aims to provide information about Fourier transform to those needing to use infrared spectroscopy, by explaining the fundamental aspects of the Fourier transform, and techniques for analyzing infrared data obtained for a wide number of materials. It summarizes the theory, instrumentation, methodology, techniques and application of FTIR spectroscopy, and improves the performance and quality of FTIR spectrophotometers.

InTech Europe
University Campus STeP Ri
Slavka Krautzeka 83/A
51000 Rijeka, Croatia
Phone: +385 (51) 770 447
Fax: +385 (51) 686 166
www.intechopen.com

InTech China
Unit 405, Office Block, Hotel Equatorial Shanghai
No.65, Yan An Road (West), Shanghai, 200040, China
中国上海市延安西路65号上海国际贵都大饭店办公楼405单元
Phone: +86-21-62489820
Fax: +86-21-62489821